International Journal of Mass Spectrometry 289 (2010) 1–5

Contents lists available at ScienceDirect

International Journal of Mass Spectrometry

journal homepage: www.elsevier.com/locate/ijms

Theoretical study of the effect of damping force on higher stability regions in a Paul trap

Iman Ziaeian, Houshyar Noshad*

Physics Department, Nuclear Science Research School, Nuclear Science and Technology Research Institute, P.O. Box 14395-836, Tehran, Iran

ARTICLE INFO

Article history:
Received 28 June 2009
Received in revised form 1 September 2009
Accepted 2 September 2009
Available online 11 September 2009

Keywords:
Damping force
Higher stability region
Paul trap

ABSTRACT

Dynamical behavior of particles in a Paul trap in the presence of damping force has been investigated. Position of trapped ions as a function of time, ion trajectories and the phase space curves considering the effect of the damping force were obtained. Four regions of stability for r and z components with the damping force as well as the maximum value of q when $U=0$ for the first region, namely q_{max}, versus damping factor k were computed using the fourth-order Runge–Kutta method. Comparisons were made with the corresponding stability diagrams without the damping force effect recently published in the literature. The third and fourth stability regions in the presence of the damping force, the curve of q_{max} as a function of k and the related equation are reported for the first time.

1. Introduction

Some techniques based on laser cooling of atoms have been seriously used for high-resolution mass spectrometry since 1985. Such study plays an important role in the dynamics of the particles confined in a quadrupole ion trap [1]. In this process, a moving atom in a Paul trap travels toward a laser beam and absorbs photons from the beam. The energy of the atom is slowed down, and consequently the atom experiences a damping force proportional to its speed. Using this technique, it is possible to cool atoms to a temperature down to a few micro-Kelvin, and confine them in a region into the trap for times long enough to carry out an experiment. Computation of ion motions in a Paul trap considering the effect of damping force as well as the corresponding stability regions are of particular importance in high-resolution mass spectrometry [2].

On the other hand, Paul traps operating in the first stability region are used for some applications. To obtain mass spectrometry with higher resolution or for specialized applications, one might design a Paul trap to operate in higher stability regions [3,4] and at very low temperature. However, these regions are not used as extensively as the first region. For higher regions, only a very small mass range of ions can be trapped, which are specified by the sizes of the stability regions [5]. For an ion with a given energy, using a trap operating in these regions, higher resolution can be achieved. In other words, for a given resolution, ions of higher kinetic energy can be trapped [4]. Paul traps working in the higher stability diagrams considering the effects of damping force gain much higher mass resolution in comparison with those operating in the first region of stability.

Influence of damping force on the motion of a single ion and the corresponding first and second stability diagrams have been investigated by Hasegawa and Uehara [6]. Moreover, one can see the stability of three-dimensional motion for a single particle in a Paul trap and the two stability diagrams in the presence of the damping force. It is worth nothing that, so far as we know, no report exists regarding the computation of stability regions higher than the second one for a Paul trap considering the damping force.

The purpose of this article is to study the dynamical behavior of ions confined in a Paul trap in the presence of the damping force as well as computation of the higher stability regions using the fourth-order Runge–Kutta method. The four diagrams of stability with the effect of damping force presented here have been compared with the corresponding regions found in the literature without the damping force. The third and fourth stability regions in the presence of the damping force have not been reported previously. Furthermore, the effect of the damping factor on the quantity q_{max} was numerically computed which has been carried out for the first time.

2. Theory

Fig. 1 shows a schematic view of a Paul trap with grounded ring electrode. The damping force F is assumed to be proportional to the velocity v of the ions as follows:

$$F = -Dv, \tag{1}$$

* Corresponding author. Tel.: +98 21 88221076.
E-mail address: hnoshad@aeoi.org.ir (H. Noshad).

1387-3806/$ – see front matter © 2009 Elsevier B.V. All rights reserved.
doi:10.1016/j.ijms.2009.09.003

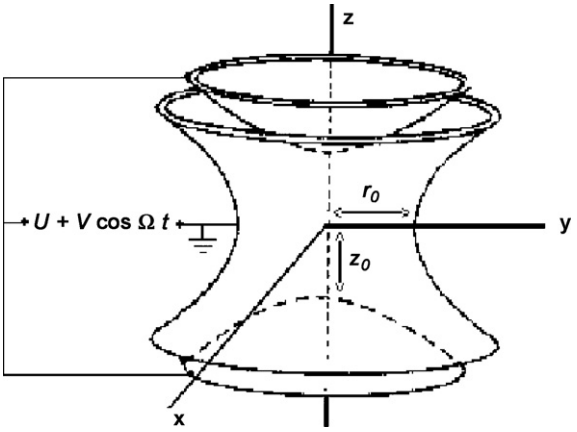

Fig. 1. A schematic view of a Paul trap.

where $D = M\gamma$ and v stands for the ion velocity. In the relation, the parameter M denotes the mass of the ion; whereas, γ is a constant. It is worth noting that there are two kind of damping forces; one is due to the collisions of ions with the buffer gas molecules into the trap; while another one is related to the collisions of ions with the photons of the laser used for cooling purposes. For collisions with gas molecules, the constant γ is extracted by the mobility data for specified ions and buffer gases into the trap, and depends on the pressure and temperature of the gas. For instance, typical data for mobility of ions with small drift velocities in some gases for a pressure of 10^{-4} mbar can be found in [7]. Moreover, the constant γ is expressed in terms of the mobility μ as follows [7]:

$$\gamma = \frac{q}{M}\frac{1}{\mu}. \tag{2}$$

The reduced mobility μ_0 is also given by the following expression [7]:

$$\mu_0 = \mu\frac{273.16\,K}{T}\frac{p}{1013\,\text{mbar}}, \tag{3}$$

where T and p are the temperature of the buffer gas in K and its pressure in mbar, respectively. As long as the kinetic energy of the ion does not exceed a few electron-volts, the mobility is usually constant within a few percent. In accordance with the simple theory of hard-sphere collisions, the mobility of the ion decreases, as the mass of the buffer gas increases.

At low pressures, collisions of ions with the photons of the laser employed for cooling of ions is a dominant phenomenon; whereas, collisions of ions with the buffer gas molecules have less contribution in the damping term.

By applying the dc and high frequency ac voltages to the end-cap electrodes of the trap, namely $U + V\cos\Omega t$, and considering $r_0^2 = 2z_0^2$ for the trap [8], solving the Laplace's equation gives the electric quadrupole potential into the trap as follows [8,9]:

$$\phi(r,z) = \frac{\left(U + V\cos\Omega t\right)}{4z_0^2}\left(2z^2 - r^2 + 2z_0^2\right), \tag{4}$$

where V stands for zero to peak voltage, namely V_{0-P}, and $\Omega = 2\pi f$ denotes the angular frequency of the ac voltage, and f is the frequency in Hz. Afterwards, the electric field components into the trap are expressed by [9]

$$E_z = -\frac{\left(U + V\cos\Omega t\right)}{z_0^2}z \tag{5}$$

$$E_r = \frac{\left(U + V\cos\Omega t\right)}{2z_0^2}r. \tag{6}$$

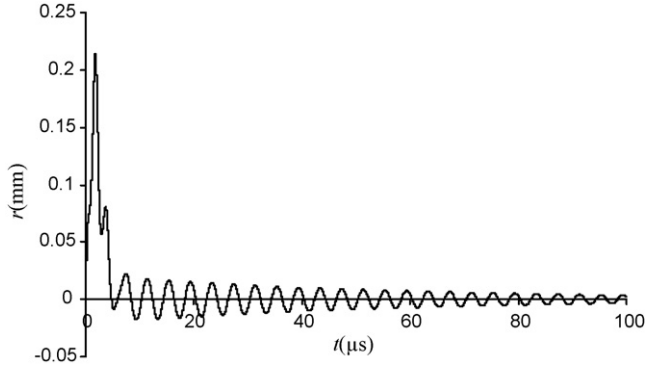

Fig. 2. The r position as a function of time in the presence of damping force ($k = 1$) for a $^{23}Na^+$ ion for $f = 0.5$ MHz, $U = 0$, $V = 310$ V and $r_0 = 15$ mm.

The set of differential equations governing the motion of an ion with mass M and charge Q into the trap taking into account the effect of damping force is given as follows:

$$\frac{d^2z}{d\xi^2} + 2k\frac{dz}{d\xi} + \left(a_z - 2q_z\cos 2\xi\right)z = 0 \tag{7}$$

$$\frac{d^2r}{d\xi^2} + 2k\frac{dr}{d\xi} + \left(a_r - 2q_r\cos 2\xi\right)r = 0. \tag{8}$$

In the relations, the dimensionless parameters a, q, ξ and damping factor k are defined as

$$a_z = -2a_r = \frac{4QU}{Mz_0^2\Omega^2} \tag{9}$$

$$q_z = -2q_r = \frac{-2QV}{Mz_0^2\Omega^2} \tag{10}$$

$$\xi = \frac{\Omega t}{2} \tag{11}$$

$$k = \frac{D}{M\Omega}. \tag{12}$$

3. Results and discussion

The set of ordinary differential Eqs. (7) and (8) were numerically solved considering damping force effect due to collisions of the ions with photons with damping factor $k = 1$. As the damping force due to photons is dominant, the quantity $k = 1$ can be attributed to any low buffer gas pressure down to 10^{-5} mbar. For a ten-fold increase in pressure, if the new pressure still becomes of the order of 10^{-5} mbar, trapping of ions occur, and our computation is valid. It goes without saying that for atmospheric pressure, there is no ion trapping.

It is worthwhile to note that Eqs. (7) and (8) were solved by Hasegawa and Uehara [6] using a transformation in order to be reduced to the Mathieu's equation [8]. In this article, our computation was numerically carried out using the fourth-order Runge–Kutta method [10]. In the algorithm, small steps for the dimensionless variable ξ were selected in order to make sure that the computational results are accurate enough.

Due to the damping factor k, the dynamical behavior of the ion may become stable, which corresponds to a bounded particle into the Paul trap. Figs. 2–5 depict the r and z positions as a function of time, the phase space curve and ion trajectory for a typical ion such as $^{23}Na^+$ obtained from our computation for a Paul trap with $r_0 = 15$ mm, $f = 0.5$ Hz, $U = 0$ and $V = 310$ V, taking into account the damping force, when $k = 1$. It is more clear that under these conditions, ion trajectories with no damping ($k = 0$), which correspond to unstable cases can become stable under heavy damping. It is worth noting that Fig. 4 is also called as a Poincaré plot.

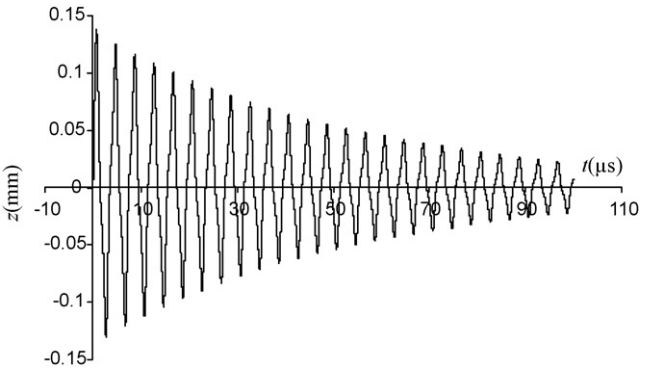

Fig. 3. The z position as a function of time in the presence of damping force ($k = 1$) for a $^{23}Na^+$ ion for $f = 0.5$ MHz, $U = 0$, $V = 310$ V and $r_0 = 15$ mm.

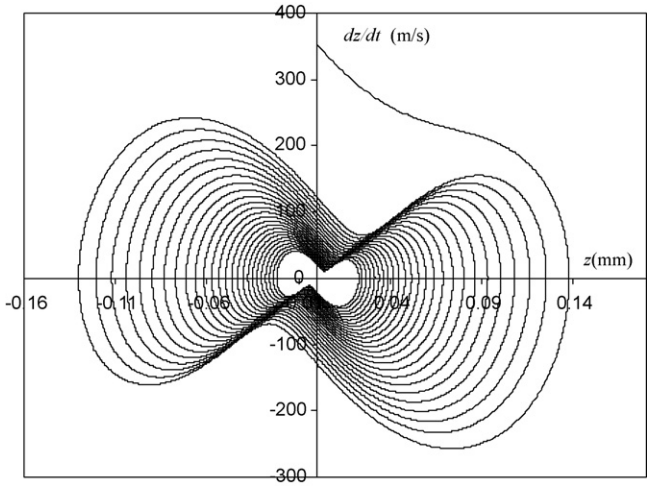

Fig. 4. dz/dt as a function of z in the presence of damping force ($k = 1$) for a $^{23}Na^+$ ion for $f = 0.5$ MHz, $U = 0$, $V = 310$ V and $r_0 = 15$ mm.

In Figs. 6 and 7 the stability regions for z and r components obtained from our computation considering the damping force ($k = 1$) have been compared with the corresponding results without the damping term, namely $k = 0$. The curves in the figures have been labeled in accordance with the terminology used by March and Hughes [11]. One can see that the even-order curves are symmetric about the a axis, but the odd-order curves are not.

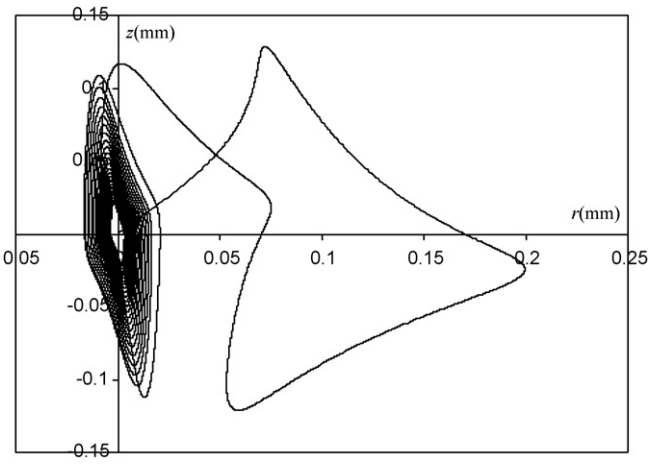

Fig. 5. The trajectory of a $^{23}Na^+$ ion in the presence of damping force ($k = 1$) for $f = 0.5$ MHz, $U = 0$, $V = 310$ V and $r_0 = 15$ mm.

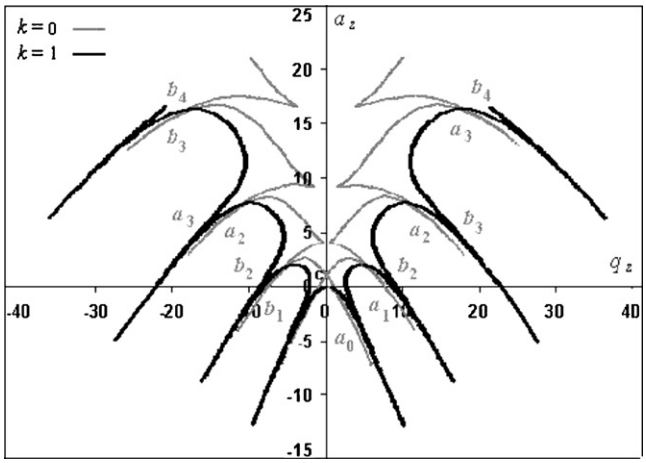

Fig. 6. Comparison between the stability regions for z component in the a–q plane with and without damping force.

Afterwards, four stability regions for the Paul trap were computed using the fourth-order Runge–Kutta method. Figs. 8–11 show the four stability regions obtained from our computational results in the presence of damping force. The corresponding results for $k = 0$ taken from [5] are also included in Figs. 8–11 in order to be able to compare them at a glance. As a conclusion, one can see that the first stability region for $k = 1$ is significantly stretched as compared with the corresponding result for $k = 0$. Whereas, the second, third and fourth stability regions are not only enlarged but also shifted. It is noticeable that the first and second stability diagrams shown in Figs. 8 and 9 are in good agreement with the results reported by Hasegawa and Uehara [6].

Computation of q_{max} is of particular importance in order to design and construction of a Paul trap. Hence, we calculated q_{max} in terms of the damping factor k. Fig. 12 represents q_{max} as a function of k. A nonlinear fitting for the curve gives Eq. (13), which is in excellent agreement with the computational data within the uncertainty of 2%.

$$q_{max} = 0.82 \exp(1.04k) \tag{13}$$

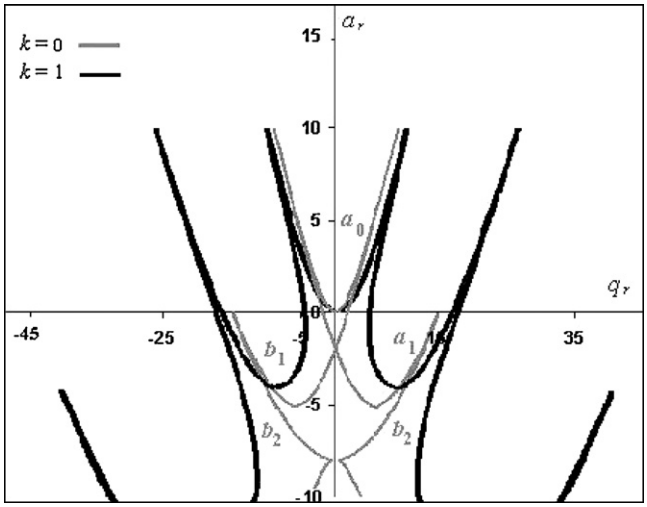

Fig. 7. Comparison between the stability regions for r component in the a–q plane with and without damping force.

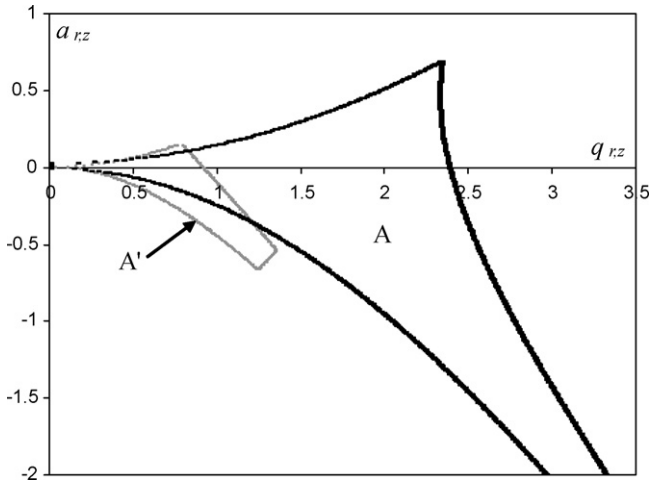

Fig. 8. The first stability region for a Paul trap in the a–q plane. The diagrams labeled by A and A′ correspond to $k = 1$ and $k = 0$, respectively.

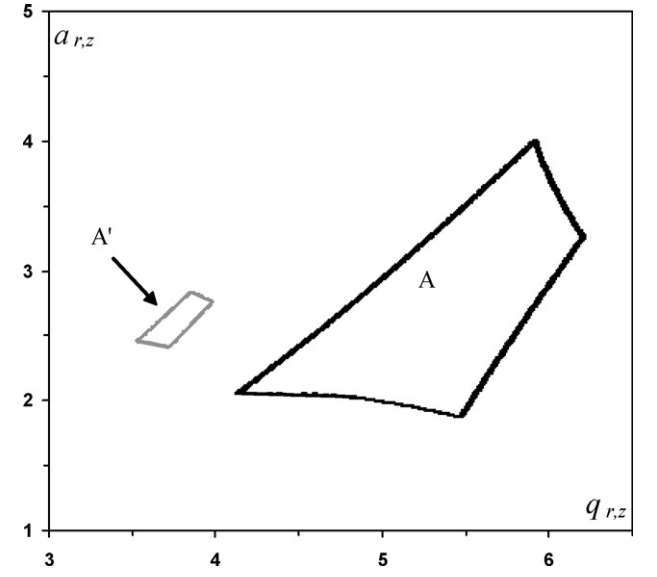

Fig. 9. The second stability region for a Paul trap in the a–q plane. The diagrams labeled by A and A′ correspond to $k = 1$ and $k = 0$, respectively.

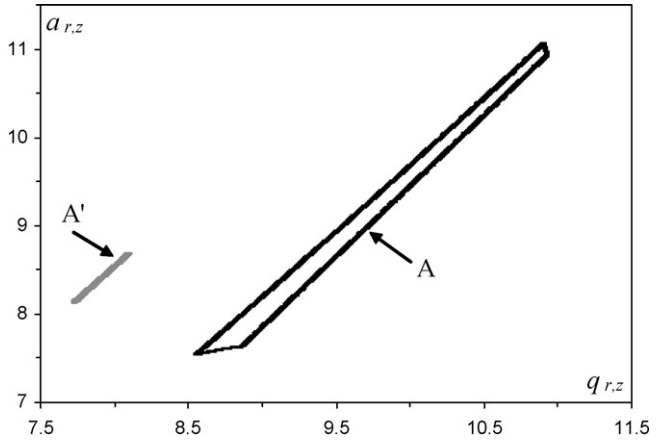

Fig. 10. The third stability region for a Paul trap in the a–q plane with A and A′ labels, which correspond to $k = 1$ and $k = 0$, respectively.

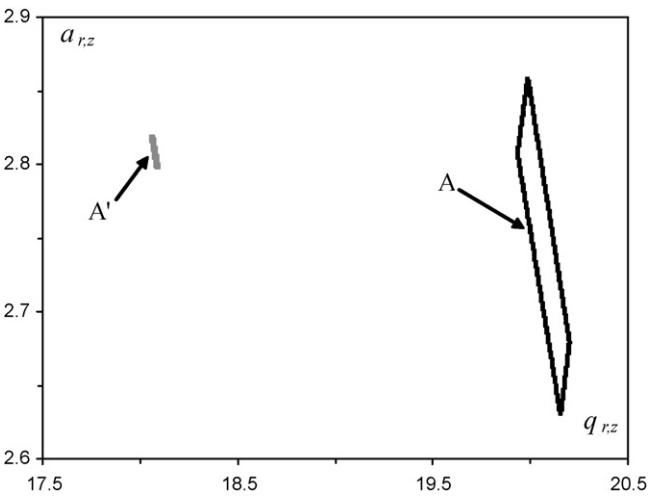

Fig. 11. The fourth stability region for a Paul trap in the a–q plane with A and A′ labels, which correspond to $k = 1$ and $k = 0$, respectively.

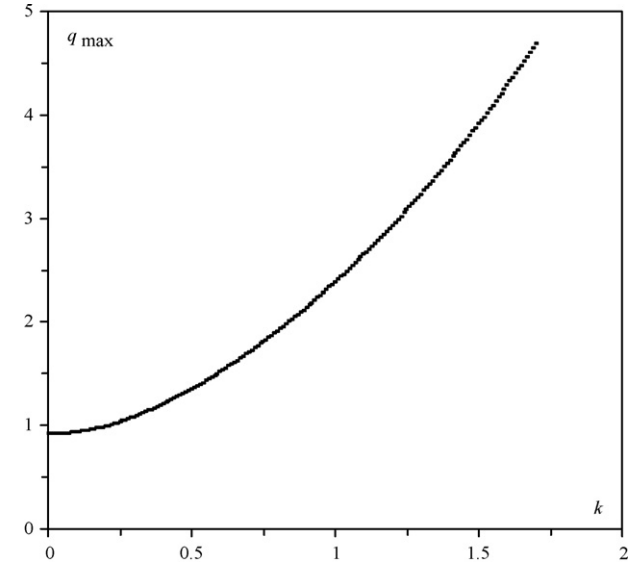

Fig. 12. q_{max} as a function of damping factor k in a Paul trap defined for the first stability region for $0 \leq k \leq 1.7$.

4. Conclusion

Four stability regions of a Paul trap in the presence of damping force were computed using an algorithm based on the fourth-order Runge–Kutta method. The r and z stability diagrams as well as the third and fourth regions of stability with damping term have been computed for the first time. We drew a conclusion that the first stability region considering damping force is enlarged in comparison with the result obtained without the damping term; whereas, for the higher regions of stability one can see a significant shift as well as enlargement.

Furthermore, for the first region, q_{max} versus damping factor for $0 \leq k \leq 1.7$ presented here gives fruitful information on ion trapping in various buffer gas pressure and temperature. We concluded that for $k > 1.7$, which corresponds to higher gas pressure into the trap, an anomalous in shape of the first region is observed. It means that the quantity q_{max} cannot be defined as a single-valued parameter. The curve q_{max} in terms of the damping factor k has not been reported in the literature previously.

References

[1] J. Eschner, G. Morigi, F. Schmidt, R. Blatt, J. Opt. Soc. Am. B 20 (2003) 1003.
[2] D.J. Wineland, W.M. Itano, R.S. van Dyck, Adv. At. Mol. Phys. 19 (1983) 135.
[3] N.V. Konenkov, M. Sudakov, D.J. Douglas, J. Am. Soc. Mass Spectrom. 13 (2002) 597.
[4] Z. Du, D.J. Douglas, N.V. Konenkov, J. Anal. Atom Spectrom. 14 (1999) 1111.
[5] H. Noshad, A. Doroudi, Int. J. Mass Spectrom. 281 (2009) 79.
[6] T. Hasegawa, K. Uehara, Appl. Phys. B: Lasers Opt. 61 (1995) 159.
[7] K. Blaum, F. Herfurth, Lecture Notes in Physics 749: Trapped Charged Particles and Fundamental Interactions, Springer, Berlin, 2008, pp. 99–100.
[8] R.E. March, J.F.J. Todd, Quadrupole Ion Trap Mass Spectrometry, second ed., Wiley, New Jersey, 2005 (chapter 2).
[9] P.H. Dawson, Quadrupole Mass Spectrometry and Its Applications, AIP, New York, 1995 (originally published in 1976 by Elsevier Publishing Company, Amsterdam).
[10] G. Wheatley, Applied Numerical Analysis, Pearson Education Inc., New Jersey, 2006.
[11] R.E. March, R.J. Hughes, Quadrupole Storage Mass Spectrometry, Wiley, New York, 1989, p. 39.